

## 9.1. INTENSITY CORRELATIONS

### 9.1.1. General Properties

The temporal profile  $I_s(t)$  of an optical signal can be easily determined, if a shorter (reference) pulse of known shape  $I_r(t)$  is available. The method is to measure the intensity cross correlation:

$$A_c(\tau) = \int_{-\infty}^{\infty} I_s(t)I_r(t - \tau) dt. \quad (9.1)$$

Let us define the Fourier transforms of the intensity profiles as:

$$\mathcal{I}_j(\Omega) = \int_{-\infty}^{\infty} I_j(t)e^{-i\Omega t} dt, \quad (9.2)$$

where the subscript  $j$  indicates either the reference ( $r$ ) or signal ( $s$ ) pulse. The Fourier transform of Eq. (9.2) should not be confused with the spectral intensity (proportional to  $|\tilde{\mathcal{E}}(\Omega)|^2$ ). The Fourier transform of the correlation (9.1) is  $A_c(\Omega)$ , related to the Fourier transforms of the intensities by:

$$A_c(\Omega) = \mathcal{I}_r(\Omega)\mathcal{I}_s^*(\Omega). \quad (9.3)$$

The shape of the signal  $I_s(t)$  can be determined by first taking the Fourier transform  $A_c(\Omega)$  of the measured cross correlation and dividing by the Fourier transform  $\mathcal{I}_r(\Omega)$  of the known reference pulse  $I_r(t)$ . The inverse Fourier transform of the complex conjugate of the ratio  $A_c(\Omega)/\mathcal{I}_r(\Omega)$  is the temporal profile  $I_s(t)$ . In presence of noise, this operation leads to large errors unless the reference function is the (temporally) shorter of the two pulses being correlated (or the function with the broadest spectrum). The ideal limit is of course that of the reference being a delta function. In the frequency domain, we are dividing by a constant. In the time domain, the shape of the correlation  $A_c(\tau)$  is identical to that of the signal  $I_s(t)$ . Even in that ideal case, the intensity cross-correlation has an important limitation: It does not provide any information on the phase content (frequency or phase modulation) of the pulse being analyzed.

### 9.1.2. The Intensity Autocorrelation

In most practical situations, a reference pulse much shorter than the signal cannot be generated. In the ideal cases where such a pulse is available, there is still a need for a technique to determine the shape of the reference signal.

It is therefore important to consider the limit where the signal itself has to be used as reference. The expression (9.1) with  $I_s(t) = I_r(t) = I(t)$  is called an intensity autocorrelation. An autocorrelation is always a symmetric function—this property can be understood from a comparison of the overlap integral for positive and negative arguments  $\tau$ . According to Eq. (9.3), the Fourier transform of the autocorrelation is a real function, consistent with a symmetric function in the time domain. As a result, the autocorrelation provides only little information on the pulse shape, because an infinity of symmetric and asymmetric pulse shapes can have similar autocorrelations. Nevertheless, the intensity autocorrelation is a widely used diagnostic technique, because it can be easily implemented, and is the first tool used to determine whether a laser is producing short pulses rather than intensity fluctuations of a continuous background. Typical examples are given in Section 9.3. The intensity autocorrelation is also used to quote a “pulse duration.” The most widely used procedure is to *assume* a pulse shape (generally a  $\text{sech}^2$  or a Gaussian shape), and to “determine” the pulse duration from the known ratio between the FWHM of the autocorrelation and that of the pulse. The parameters pertaining to the various shapes are listed in Table 9.1 in Section 9.4.

### 9.1.3. Intensity Correlations of Higher Order

Let us look at an intensity correlation of a higher order, defined as:

$$A_n(\tau) = \int_{-\infty}^{\infty} I(t)I^n(t - \tau)dt. \quad (9.4)$$

For  $n > 1$ , the function defined by Eq. (9.4) has the same symmetry as the pulse. In fact, for a reasonably peaked function  $I(t)$ ,  $\lim_{n \rightarrow \infty} I^n(t) \propto \delta(t)$ , and the shape of the correlation  $A_n(\tau)$  approaches the pulse shape  $I(t)$ . Such higher-order correlations are convenient and powerful tools to determine intensity profiles.

## 9.2. INTERFEROMETRIC CORRELATIONS

### 9.2.1. General Expression

We have analyzed in Chapter 2 the Michelson interferometer and defined the field<sup>1</sup> correlation measured by that instrument as:

$$G_1(\tau) = \tilde{A}_{12}^+(\tau) + c. c = \frac{1}{4} \int_{-\infty}^{\infty} \tilde{\mathcal{E}}_1(t)\tilde{\mathcal{E}}_2^*(t - \tau)e^{i\omega_e\tau} dt + c. c. \quad (9.5)$$

<sup>1</sup>The field correlation is often referred to as a first-order correlation.

We have seen also that the Fourier transform of  $A_{12}^+(\tau)$  is equal to  $\tilde{E}_1^*(\Omega)\tilde{E}_2(\Omega)$  [Eq. (2.6)]. Hence, the Fourier transform of the autocorrelation (identical fields) is proportional to the spectral intensity of the pulse. Therefore, a first-order field autocorrelation does not carry any other information than that provided by a spectrometer.

In a Michelson interferometer, let us add to the detector a second harmonic generating crystal (type I) and a filter to eliminate the fundamental. Instead of the expression (9.5), the detected signal is a second-order interferometric correlation, proportional to the function:

$$G_2(\tau) = \int_{-\infty}^{\infty} \langle |E_1(t-\tau) + E_2(t)|^2 \rangle dt. \quad (9.6)$$

Here  $\langle \rangle$  denotes averaging over the fast oscillations of the electric field and the integral stands for integration over the pulse envelope. A Mach-Zehnder interferometer can also be substituted for a Michelson interferometer for such a measurement [2]. Replacing the fields by the usual envelope and phase functions,  $E_{1,2} = (\mathcal{E}_{1,2}e^{i\omega_\ell t}e^{i\varphi_{1,2}} + c. c.)/2$  and performing the  $\langle \rangle$  average yields for the correlation apart from a constant factor:

$$G_2(\tau) = A(\tau) = A_0(\tau) + \text{Re} [A_1(\tau)e^{-i\omega_\ell \tau}] + \text{Re} [A_2(\tau)e^{-2i\omega_\ell \tau}], \quad (9.7)$$

where

$$A_0(\tau) = \int_{-\infty}^{\infty} [\mathcal{E}_1^4(t-\tau) + \mathcal{E}_2^4(t) + 4\mathcal{E}_1^2(t-\tau)\mathcal{E}_2^2(t)] dt \quad (9.8)$$

$$A_1(\tau) = 4 \int_{-\infty}^{\infty} \mathcal{E}_1(t-\tau)\mathcal{E}_2(t) [\mathcal{E}_1^2(t-\tau) + \mathcal{E}_2^2(t)] e^{i[\varphi_1(t-\tau) - \varphi_2(t)]} dt \quad (9.9)$$

$$A_2(\tau) = 2 \int_{-\infty}^{\infty} \mathcal{E}_1^2(t-\tau)\mathcal{E}_2^2(t) e^{2i[\varphi_1(t-\tau) - \varphi_2(t)]} dt. \quad (9.10)$$

The purpose of the decomposition (9.7) is to show that the correlation has three frequency components<sup>2</sup> centered respectively around zero frequency, around  $\omega_\ell$  and  $2\omega_\ell$ . Most often, the detection system of the correlator will act as a low pass filter, eliminating all but the first term of the expansion. The interferometric correlation reduces then to  $A_0(\tau)$ —the sum of a background term and the

<sup>2</sup>Here “frequency” refers to the variation of the function  $G_2(\tau)$  as a function of its argument  $\tau$ . The latter argument  $\tau$  is the delay parameter, which is continuously tuned in the correlation measurement.

(background-free) intensity correlation [labeled  $A_c(\tau)$  in Eq. (9.1)]. The terms  $A_0$ ,  $A_1$ , and  $A_2$  of the expansion (9.7) can be extracted from a measurement by taking the Fourier transform of the data, identifying the cluster of data near the three characteristic frequencies, and recovering them by successive inverse Fourier transforms. Fast data acquisition and processing can also perform this task in real time when working with fs oscillators [3]. The components  $A_1$  and  $A_2$  contain phase terms  $[\varphi_1(t - \tau) - \varphi_2(t)]$ , and thus carry information about pulse chirp.

Similarly the third-order interferometric correlation

$$G_3(\tau) = B(\tau) = \int \left\langle \left| [E_1(t - \tau) + E_2(t)]^3 \right|^2 \right\rangle dt \quad (9.11)$$

has four frequency components. In terms of pulse envelopes and phases it can be written as

$$B(\tau) = B_0(\tau) + \text{Re} [B_1(\tau)e^{-i\omega_\ell\tau}] + \text{Re} [B_2(\tau)e^{-2i\omega_\ell\tau}] + \text{Re} [B_3(\tau)e^{-3i\omega_\ell\tau}], \quad (9.12)$$

where

$$B_0(\tau) = \int \left\{ \mathcal{E}_1^6(t - \tau) + \mathcal{E}_2^6(t) + 9\mathcal{E}_1^2(t - \tau)\mathcal{E}_2^2(t) [\mathcal{E}_1^2(t - \tau) + \mathcal{E}_2^2(t)] \right\} dt \quad (9.13)$$

$$B_1(\tau) = 6 \int \left[ \mathcal{E}_1^4(t - \tau) + \mathcal{E}_2^4(t) + 3\mathcal{E}_1^2(t - \tau)\mathcal{E}_2^2(t) \right] \times \mathcal{E}_1(t - \tau)\mathcal{E}_2(t) e^{i[\varphi_1(t - \tau) - \varphi_2(t)]} dt \quad (9.14)$$

$$B_2(\tau) = 6 \int \left[ \mathcal{E}_1^2(t - \tau) + \mathcal{E}_2^2(t) \right] \mathcal{E}_1^2(t - \tau)\mathcal{E}_2^2(t) e^{2i[\varphi_1(t - \tau) - \varphi_2(t)]} dt \quad (9.15)$$

$$B_3(\tau) = 2 \int \mathcal{E}_1^3(t - \tau)\mathcal{E}_2^3(t) e^{3i[\varphi_1(t - \tau) - \varphi_2(t)]} dt. \quad (9.16)$$

Again we have omitted a constant factor. The zero frequency component of this interferometric correlation,  $B_0(\tau)$ , corresponds to the third-order intensity correlation with background.

## 9.2.2. Interferometric Autocorrelation

### 9.2.2.1. General Properties

Let us consider in more detail the particular case of the previous expressions for the cross correlation (9.6) through (9.10) where the two fields  $E_1 = E_2 = E$ . At  $\tau = 0$ , the peak value of the function  $A(\tau = 0) = 16 \int \mathcal{E}^4(t)dt$ . For large delays compared to the pulse duration, cross products containing terms with  $\mathcal{E}(t - \tau)\mathcal{E}(t)$  vanish, leaving a background of  $A(\tau = \infty) = 2 \int \mathcal{E}^4(t)dt$ . The peak to background ratio for the interferometric autocorrelation is thus 8 to 1. The “d.c.” term of the interferometric autocorrelation,  $A_0(\tau)$ ,—which is in fact an intensity autocorrelation—has a peak to background of 3 to 1. The measurement leading to  $A_0(\tau)$  is generally referred to as the *intensity autocorrelation with background*, as opposed to the *background free autocorrelation* leading to the expression  $A_c(\tau)$  (9.1).

The fourth term of the expansion of Eq. (9.7) can be regarded as a correlation of the second harmonic fields. In the absence of phase modulation—i.e., for bandwidth-limited pulses—this function is identical to the intensity autocorrelation. This property has been exploited to determine if a pulse is phase modulated or not [4].

As any autocorrelation, the interferometric autocorrelation is a symmetric function. However, as opposed to the intensity autocorrelation, it contains phase information. The shape and phase sensitivity of the interferometric autocorrelation can be exploited to:

1. *qualitatively* test the absence or presence of phase modulation and eventually determine the type of modulation;
2. quantitatively measure a *linear* chirp; and
3. determine, in combination with the pulse spectrum and linear filtering, the pulse shape and phase by fitting procedures (see Section 9.4).

### 9.2.2.2. Linearly Chirped Pulses

The sensitivity of the interferometric autocorrelation to chirp is well illustrated by the experimental recordings made with the beam from a Ti:sapphire laser in Spence *et al.* [5]. The lower and upper envelopes of the interference pattern split evenly from the background level in Figure 9.1 pertaining to an unchirped 45 fs pulse. In the case of a phase modulated pulse as in Figure 9.2, the interference pattern is much narrower than the pulse intensity autocorrelation. The wings of the interferometric autocorrelation are identical to those of the intensity autocorrelation. The level at which the interference pattern starts relative to the peak (2.8/8 in the case of Fig. 9.2) is a measure of the chirp, as explained later.

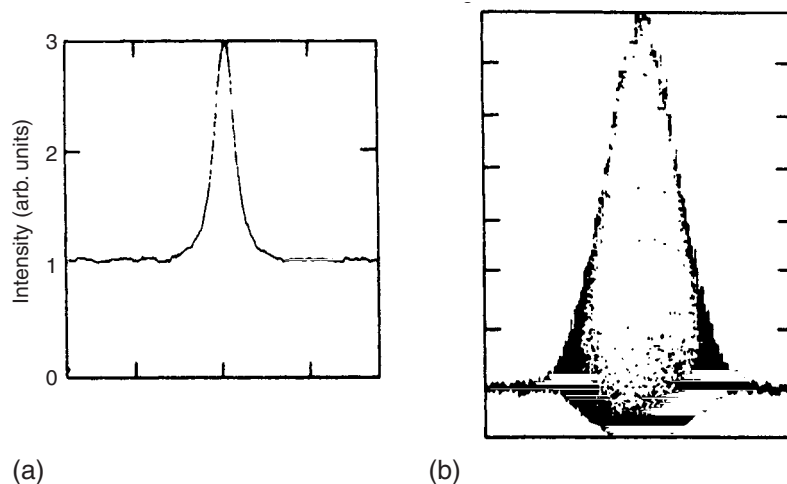


**Figure 9.1** Intensity (with background) (a) and interferometric (b) autocorrelation traces of a mode-locked Ti:sapphire laser pulse after extracavity pulse compression. Note the peak to background ratios of 3/1 and 8/1 for the intensity and interferometric autocorrelations, respectively (from Spence *et al.* [5]).

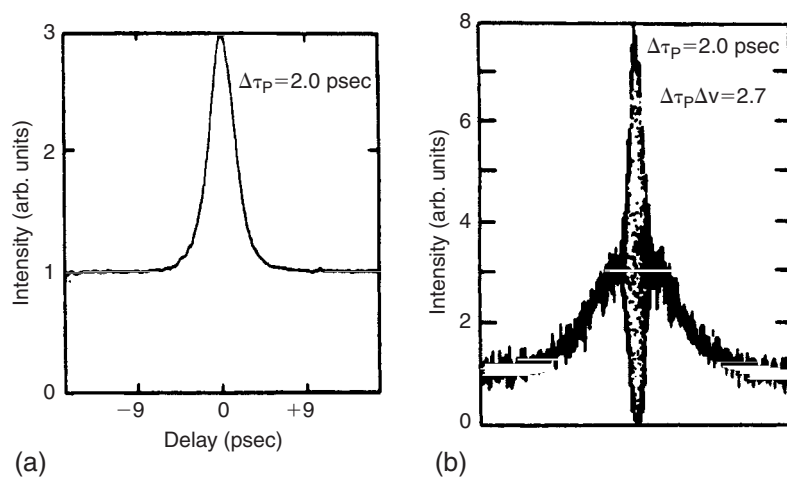


**Figure 9.2** Intensity (a) and interferometric (b) autocorrelation traces of a mode-locked phase modulated Ti:sapphire laser pulse (from Spence *et al.* [5]).

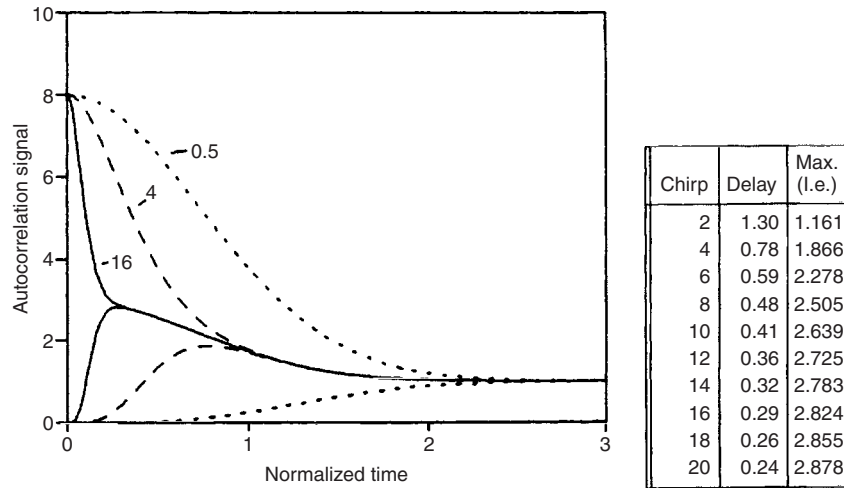


**Figure 9.3** Interferometric autocorrelations of Gaussian pulses  $\tilde{E}(t) = \exp\{-(1 + ia)(t/\tau_G)^2\}$  for various values of the linear chirp parameter  $a$ . The upper and lower envelopes of the autocorrelations are plotted for three values of the chirp parameter  $a$ . The upper and lower envelopes merge with the intensity autocorrelation. The table on the right shows the position (delay and value) of the maxima of the lower envelope (l.e.) of the interferometric autocorrelation as a function of chirp parameter  $a$ .

A simple tabulation of the chirp can be made by considering a linearly chirped Gaussian pulse ( $\tilde{E}(t) = \exp[-(1 + ia)(t/\tau_G)^2]$ ), for which the interferometric autocorrelation can be determined analytically:

$$G_2(\tau) = \left\{ 1 + 2 \exp \left[ - \left( \frac{\tau}{\tau_G} \right)^2 \right] + 4 \exp \left[ - \frac{a^2 + 3}{4} \left( \frac{\tau}{\tau_G} \right)^2 \right] \cos \left[ \frac{a}{2} \left( \frac{\tau}{\tau_G} \right)^2 \right] \right. \\ \left. \times \cos(\omega_\ell \tau) + \exp \left[ -(1 + a^2) \left( \frac{\tau}{\tau_G} \right)^2 \right] \cos 2\omega_\ell \tau \right\}. \quad (9.17)$$

A graphical representation of the upper and lower envelopes as a function of the chirp parameter  $a$  is shown in Figure 9.3. Comparison of Figs. 9.2 and 9.3 indicate a chirp parameter of roughly  $a = 20$  for the experimental pulse. This is of course only an approximation, but it gives a good estimate of the magnitude of the frequency modulation near the pulse center.